5-1-2020

TESS observations of pulsating subdwarf B stars: extraordinarily short-period gravity modes in CD−28° 1974

Michael D. Reed
Missouri State University

K. A. Shoaf
MSU Underraduate

P. Nemeth

J. Vos

M. Uzundag

See next page for additional authors

Recommended Citation

Reed, M. D., K. A. Shoaf, P. Németh, J. Vos, M. Uzundag, A. S. Baran, S. K. Sahoo, C. S. Jeffery, J. H. Telting, and R. H. Østensen. "TESS observations of pulsating subdwarf B stars: extraordinarily short-period gravity modes in CD− 28° 1974." Monthly Notices of the Royal Astronomical Society 493, no. 4 (2020): 5162-5169.

Authors

Michael D. Reed, K. A. Shoaf, P. Nemeth, J. Vos, M. Uzundag, A. S. Baran, S. Saho, C. S. jeffery, J. H. Telting, and R. H. Ostensen

Monthly Notices
of the
ROYAL ASTRONOMICAL SOCIETY

MNRAS **493,** 5162–5169 (2020)
Advance Access publication 2020 March 9

doi:10.1093/mnras/staa661

TESS observations of pulsating subdwarf B stars: extraordinarily short-period gravity modes in CD−28° 1974

M. D. Reed [1,2★] K. A. Shoaf,[1] P. Németh [3,4] J. Vos,[5,6] M. Uzundag,[4] A. S. Baran [2] S. K. Sahoo,[2,7] C. S. Jeffery [8] J. H. Telting[2,9] and R. H. Østensen[1]

[1]*Department of Physics, Astronomy and Materials Science, Missouri State University, 901 S. National, Springfield, MO 65897, USA*
[2]*ARDASTELLA Research Group, Department of Physics, Pedagogical University of Cracow, ul. Podchorążych 2, PL-30-084 CraCów, Poland*
[3]*Astronomical Institute of the Czech Academy of Sciences, Fričova 298, CZ-251 65 Ondřejov, Czech Republic*
[4]*Astroserver.org, 8533 Malomsok, Hungary*
[5]*Instituto de Física y Astronomía y Centro de Astrofísica de Valparaíso, Blanco 951, Valparaiso, Chile*
[6]*Institut für Physik und Astronomie, Universität Potsdam, Haus 28, Karl-Liebknecht-Straße 24/25, D-14476 Potsdam-Golm, Germany*
[7]*Nicolaus Copernicus Astronomical Centre of the Polish Academy of Sciences, ul. Bartycka 18, PL-00-716 Warsaw, Poland*
[8]*Armagh Observatory and Planetarium, College Hill, Armagh BT61 9DG, UK*
[9]*Nordic Optical Telescope, Rambla José Ana Fernández Pérez 7, E-38711 Breña Baja, Spain*

Accepted 2020 March 3. Received 2020 March 2; in original form 2019 December 18

ABSTRACT

Transiting Exoplanet Survey Satellite (*TESS*) observations show CD−28° 1974 to be a gravity(g)-mode-dominated hybrid pulsating subdwarf B (sdBV) star. It shows 13 secure periods that form an $\ell = 1$ asymptotic sequence near the typical period spacing. Extraordinarily, these periods lie between 1500 and 3300 s, whereas typical $\ell = 1$ g modes in sdBV stars occur between 3300 and 10 000 s. This indicates a structure somewhat different from typical sdBV stars. CD−28° 1974 has a visually close F/G main-sequence companion 1.33 arcsec away, which may be a physical companion. *Gaia* proper motions indicate a comoving pair with the same distance. A reanalysis of Ultraviolet and Visual Echelle Spectrograph (UVES) spectra failed to detect any orbital motion and the light curve shows no reflection effect or ellipsoidal variability, making an unseen close companion unlikely. The implication is that CD−28° 1974 has become a hot subdwarf via single star or post-merger evolution.

Key words: stars: oscillations – subdwarfs.

1 INTRODUCTION

The *Transiting Exoplanet Survey Satellite* (*TESS*; Ricker et al. 2016) is a set of four 100-mm aperture cameras aboard a spacecraft with a highly eccentric, lunar-resonance Earth orbit. The orbit requires the telescope to change pointing roughly every lunar month. *TESS*'s main mission is to detect exoplanets via the transit method (Ricker 2015), but as it is staring at stars for a month at a time, its secondary mission is asteroseismology. In that regard, continuous, 2 min cadence, single-instrument observations cannot be matched by ground-based observatories. This makes *TESS* an excellent instrument for asteroseismology.

Asteroseismology uses stellar pulsations, which *TESS* views as periodic light variations, to discern stellar structure and evolution. Observationally, our goal is to associate periodicities with pulsation *modes* that are described by quantized spherical harmonics.

In this paper, we analyse data for a pulsating subdwarf B (sdBV) star. Subdwarf B (sdB) stars are extreme horizontal branch stars of roughly half a solar mass and 20 per cent the radius of our Sun (for a review of sdB stars, see Heber 2016). The *Kepler* mission provided transformative data for sdBV stars, in that prior to *Kepler* data, it was rare to have observationally constrained mode identifications, but from *Kepler* data, identifications are routinely determined (e.g. Reed et al. 2011; Baran et al. 2012; Telting et al. 2014). The main methods to associate periodicities with modes are frequency multiplets, where azimuthal degeneracy is lifted, typically by rotation (e.g. Baran et al. 2012), and g-mode asymptotic period sequences, where g (gravity) mode overtones (relative n) are evenly spaced in period for each degree, ℓ (see Reed et al. 2018, for a review).

We examine *TESS* data on the sdB star CD−28° 1974 [with *TESS* Identification Catalogue (TIC) number 13145616 also HE 0505−2806 and GALEX J0507−2802]. CD−28° 1974 is involved in a complex system of nearby stars, one of which may be a physical companion. Previous spectroscopic observations of CD−28° 1974 have identified it as a spectroscopic binary with an F- or G-type companion (Vennes, Kawka & Németh 2011). Low-dispersion spectra obtained and fitted by Vennes et al. (2011) determined $T_{\rm eff} = 25\,000 \pm 2500$ K, $\log g = 4.90 \pm 0.35$ dex (cgs), and $\log n({\rm HE})/n({\rm H}) = -2.2 \pm 0.5$. Németh, Kawka &

★ E-mail: mikereed@missouristate.edu

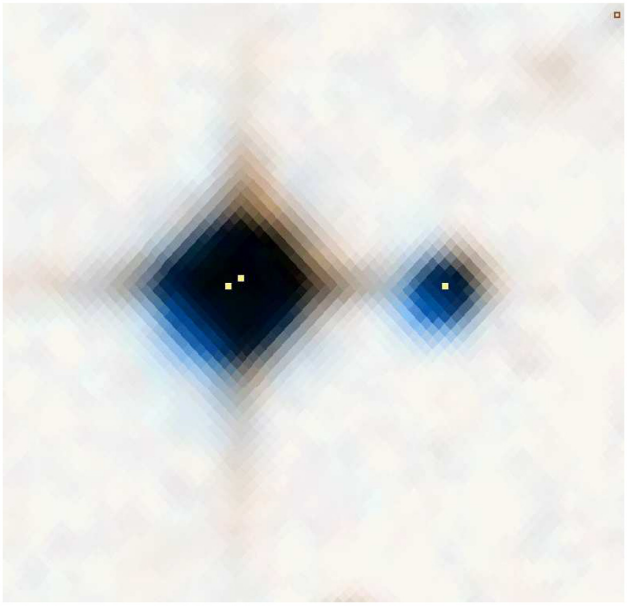

Figure 1. Digitized Sky Survey image of the CD−28° 1974 field, 1.5 arcmin on a side. The *Gaia* Data Release 2 (DR2) positions are marked with squares.

Vennes (2012) obtained three low-resolution spectra, from which they found 'changing composite features'. From their individual spectra they produced wildly differing results from $T_{\rm eff} = 25\,710^{+3450}_{-1450}$ K, $\log g = 5.28^{+0.40}_{-0.26}$ to $T_{\rm eff} = 29\,840^{+180}_{-200}$ K, $\log g = 5.61^{+0.03}_{-0.06}$. Németh et al. (2012) also write that the inspection of the field around CD−28° 1974 and the symmetry of the point spread function (PSF) profile implied crowding. The composite spectrum is most probably the result of contamination from a nearby, but independent star. Vos et al. (2018b) resolved the two stars in imaging, but not in their Ultraviolet and Visual Echelle Spectrograph (UVES) spectra and concluded that the main-sequence (MS) star was a 'foreground wide binary containing at least one MS F- or G-type star'. These differing results make CD−28° 1974's binary status enigmatic. Outside of the unresolved pair, there is another star 15 arcsec away. In Fig. 1, we show a 1.5 arcmin^2 Digitized Sky Survey image with the *Gaia* positions marked. CD−28° 1974's binary status will be discussed further in Section 3.

2 ANALYSES OF *TESS* DATA

2.1 Light-curve processing and pulsation detection

CD−28° 1974 was observed as one of our Guest Investigator (GI) program (G011177) targets, as well as a *TESS* Asteroseismic Science Consortium (TASC) target. We downloaded the processed light curve from the Mikulski Archive for Space Telescopes as a GI bulk download and used the simple aperture photometry that is not flux corrected for contamination of nearby stars. CD−28° 1974 was observed during S5 that spanned about 26 d from 2018 November 15 to 2018 December 11 and from which we used 17 421 2-min-cadence data points after σ clipping at 4σ. Our final data set was spline fitted to remove trends >1.5 d, though we also examined a non-fitted set to search for binary variations. As *TESS* has 21 arcsec pixels, there will certainly be contamination from the nearby star, in addition to the companion. This will reduce pulsation amplitudes as we normalize them as $\Delta I/\langle I\rangle$, where $\langle I\rangle$ is the average intensity. We do not attempt any flux corrections as absolute amplitudes are not important to our analyses and we report amplitudes in parts-per-thousand (ppt). The data have a temporal resolution of $1.5/T = 0.68$ μHz and we used a 4σ detection limit, calculated in pulsation-free regions of 55–115, 320–375, and 605–720 μHz and linearly interpolated in between.

The processed light curve was Fourier transformed (FT; top panel of Fig. 2) and subsequently converted to period transformed (PT; bottom panel of Fig. 2) to highlight asymptotic sequences. We non-linear least-squares (NLLS) fitted the light curve using frequencies and amplitudes from the FT as initial estimates. The fits were then removed (pre-whitened) from the light curve and reviewed by eye as a measure of goodness-of-fit. The pre-whitened FT is shown in the middle panel of Fig. 2. We pre-whitened 13 periodicities above the 4σ detection limit and four further periodicities below it (discussed below). We note that while f1 has an NLLS-fitted amplitude below 4σ, the original amplitude was over the detection threshold, and therefore we consider it intrinsic to CD−28° 1974. The resultant frequencies (periods), amplitudes, and signal-to-noise ratios (S/N) are provided in Table 1.

2.2 Pulsation mode identification

Non-radial pulsations may be described using spherical harmonics characterized by quantum numbers n, ℓ, and m. In this case n represents the number of radial nodes, ℓ the number of nodes along the surface, and m the number of azimuthal surface modes (Aerts, Christensen-Dalsgaard & Kurtz 2010). As discovered by Reed et al. (2011) using *Kepler* data, nearly all g-mode sdBV stars have asymptotic period sequences with $\ell = 1$ spacings near 250 s. As is typical, we used a Kolmogorov–Smirnov (KS) test to search for the period spacing. The results are shown in the left-hand panel of Fig. 3, an indicate a period spacing near 270 s. We then folded the periods over that spacing into an échelle diagram (right-hand panel of Fig. 3) and also used a linear regression to fit the periods. The resultant period spacing is 268.85 ± 0.32 s. CD−28° 1974's échelle diagram has a slight 'hook' in the lower portion of the sequence, which is a feature seen in other sdBV stars (Baran & Winans 2012), though usually between 3000 and 6000 s. From this sequence we were able to identify eight significant frequencies as $\ell = 1$ and another two as $\ell = 2$ from the relationship $\Pi_{\ell=2} = \Pi_{\ell=1}/\sqrt{3}$.

We noticed several peaks that appeared just under the detection threshold. We tested if their periods fit into the asymptotic sequences (to within 10 per cent), and if they did, we attempted NLLS fitting and pre-whitening. If that succeeded, we list them in Table 1 as *suggested* periodicities. These suggested periodicities were not used in the asymptotic sequence fit. We note that s1 is possibly below the acoustic cut-off, but see no harm in listing it, as it was not used to determine the asymptotic sequence. (It is also not shown in Fig. 3.)

We also searched for frequency multiplets to indicate rotation, but found none. This is not surprising as the *TESS* sector campaigns, while wonderful compared to what can be obtained from the ground, are mostly too short compared with known sdB rotation periods of tens of days (Reed et al. 2018).

2.3 Contributions from the nearby star

Previous studies have determined that the unresolved stellar companion to CD−28° 1974 is an F/G MS star, which we confirm in Section 3. These stars can also pulsate and so it is prudent to ascertain if the pulsations we detect are intrinsic to the sdB star, or

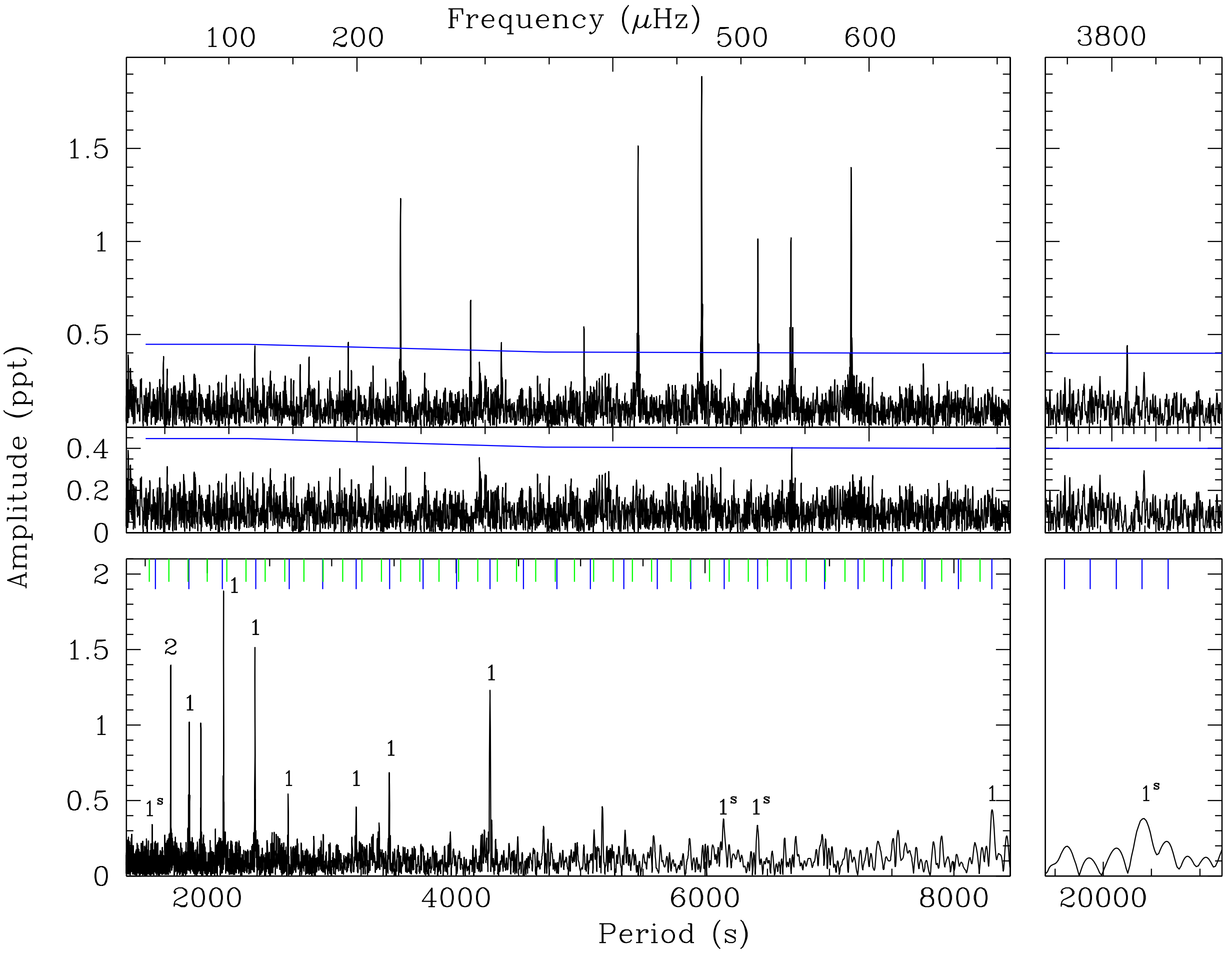

Figure 2. Fourier transform (top) and residuals after pre-whitening (middle) including the detection limit as a horizontal line. The bottom panels show the period transform. Labels identify the pulsations and the asymptotic sequences are indicated by lines (blue for $\ell = 1$ and green for $\ell = 2$) along the top. Peaks denoted with an 's' are below our detection limit (noted in Table 1 with 's' identifiers).

Table 1. Pulsations detected in CD−28° 1974. Identified periods are all $\ell = 1$ modes except for f11 and f12, which are $\ell = 2$ (and indicated with a †). Column 6 lists the relative radial order n. Column 7 lists the fractional deviation from the asymptotic sequence. Periodicities identified with an 's' are below the detection threshold and are therefore *suggested* frequencies.

ID	Freq (μHz)	Period (s)	Amp (ppt)	S/N	n	DP/P (%)
s1	48.981 (55)	20416.25 (22.97)	0.385 (88)	3.35	75	4.8
f1	120.383 (48)	8306.83 (3.34)	0.438 (88)	3.81	30	0.6
s2	155.753 (64)	6420.43 (2.65)	0.330 (88)	3.01	23	− 1.1
s3	162.627 (56)	6149.03 (2.13)	0.377 (88)	3.44	22	− 2.0
f2	193.240 (46)	5174.91 (1.24)	0.460 (88)	4.26	–	–
f3	234.083 (17)	4271.98 (0.31)	1.232 (88)	11.65	15	− 0.2
f4	288.818 (31)	3462.38 (0.37)	0.685 (88)	6.60	12	− 1.4
f5	312.830 (46)	3196.63 (0.47)	0.466 (88)	4.61	11	− 0.2
f6	377.377 (41)	2649.87 (0.29)	0.542 (91)	5.37	9	− 3.6
f7	419.559 (14)	2383.45 (0.08)	1.521 (91)	15.03	8	− 2.7
f8	469.215 (12)	2131.22 (0.05)	1.894 (91)	18.84	7	3.5
f9	513.128 (22)	1948.83 (0.08)	1.019 (91)	10.19	–	–
f10	538.930 (23)	1855.53 (0.08)	0.994 (92)	9.94	6	1.0
f11	540.361 (49)	1850.62 (0.17)	0.461 (92)	4.61	11†	3.0
f12	585.958 (16)	1706.61 (0.05)	1.401 (91)	14.06	10†	10.3
s4	642.381 (65)	1556.71 (0.16)	0.341 (91)	3.42	5	− 10.2
f13	3807.044 (48)	262.67 (4)	0.438 (87)	4.39	–	–

the F/G star. Possible pulsation types include δ Scuti, γ Dor, and solar-like oscillations.

γ Dor-type oscillations can readily be ruled out as γ Dor stars are hotter than our determination (see Table 2) and the periods are much longer than observed in CD−28° 1974, typically near 1 d (e.g. figs 1–3 of Balona et al. 2011).

δ Scuti and solar-like oscillations are p-mode pulsators, which have asymptotic sequences in frequency, rather than period. We do not readily see any frequency sequences in Table 1. δ Scuti stars would also be on the very hot end of allowable temperatures from Table 2 and also have frequencies well below those we observe (e.g. Balona, Daszyńska-Daszkiewicz & Pamyatnykh 2015).

Scaling relations exist for solar-like oscillations from which the observables $\Delta\nu$ and $\nu_{\rm max}$ can be predicted (equations 43 and 44 of García & Ballot 2019). Using $R/R_\odot$ and $T_{\rm eff}$ from Table 2 and a generous mass range of 0.85–1.8$M/M_\odot$ for F/G stars, we can determine a range for $\Delta\nu$ and $\nu_{\rm max}$ of 91–133 and 1780–3775 μHz, respectively. As the frequencies in CD−28° 1974 span 600 μHz, it is possible to make a very rough asymptotic sequence with s1, s2, f4, f6, f8, f11, and s4. The average $\Delta\nu$ is ≈99 μHz, but creating an échelle diagram with $\Delta\nu$ and ν shows no characteristic ridges of frequencies (e.g. fig. 13 of García & Ballot 2019). This is expected, as sdBV asymptotic sequences are in period ($\Delta\Pi$) rather than frequency ($\Delta\nu$). More telling is the range of $\nu_{\rm max}$,

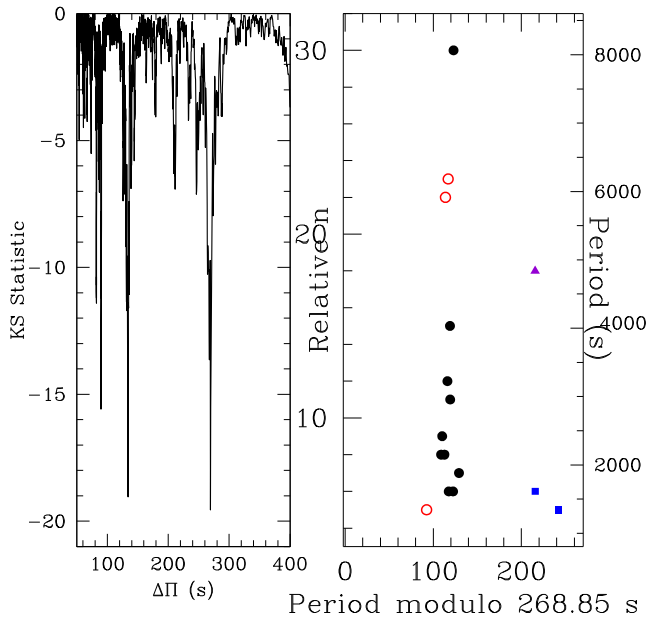

Figure 3. KS test (left) showing the $\ell = 1$ spacing near 270 s, and its overtone near 135 s. The échelle diagram (right) indicating the dominant $\ell = 1$ asymptotic sequence (black circles). Open (red) circles indicate periods below the detection limit, (blue) squares indicate periods identified as $\ell = 2$, and the (purple) triangle indicates the unidentified mode. We do not show s1 as it would compress most of the periods to the bottom of the figure.

Table 2. Parameters from *Gaia*, spectroscopy, and SED fitting.

Parameter	Value	Source
	sdB	
d (pc)	400 (13)	*Gaia*
$\mu_{\rm RA}$ (mas yr^{-1})	6.12 (11)	*Gaia*
$\mu_{\rm Dec.}$ (mas yr^{-1})	9.33 (14)	*Gaia*
log g (dex; cgs)	5.55 ± 0.09	UVES spectrum
$T_{\rm eff}$ (kK)	$29.6^{+0.38}_{-0.15}$	UVES spectrum
$T_{\rm eff}$ (kK)	24.7 (4.0)	SED
$R/{\rm R}_\odot$	0.27 (4)	SED
	MS companion	
d (pc)	391 (5)	*Gaia*
$\mu_{\rm RA}$ (mas yr^{-1})	6.42 (4)	*Gaia*
$\mu_{\rm Dec.}$ (mas yr^{-1})	9.61 (5)	*Gaia*
log g (dex; cgs)	4.00 (25)	UVES spectrum
$T_{\rm eff}$ (kK)	5.5 (3)	UVES spectrum
$T_{\rm eff}$ (kK)	5.43 (15)	SED
$R/{\rm R}_\odot$	1.23 (5)	SED

within which CD−28° 1974 has *no* frequencies. If we invert the $\nu_{\rm max}$ scaling relation, we can determine $M/{\rm M}_\odot$ using our highest amplitude frequency (f8) as $\nu_{\rm max}$. This calculation results in $M/{\rm M}_\odot \approx 0.22$, which clearly is an unrealistic value.

As such we conclude that the variability is from pulsations in the sdB star and not an F/G star.

3 SPECTROSCOPIC AND BINARY ANALYSIS

3.1 Spectral analyses

From the ESO archive we downloaded five high-resolution spectra obtained with the UVES spectrograph at the Very Large Telescope (VLT)-UT2 telescope. These spectra were taken over a period of 800 d. Radial velocities were determined using a cross-correlation with a template spectrum. For the sdB component we used a TMAP spectrum with $T_{\rm eff} = 28\,000$ K and log $g = 5.5$ and for the cool companion a G-type ATLAS local thermodynamic equilibrium (LTE) spectrum (Kurucz 1979) was used. For more details on the radial velocity determination, see Vos et al. (2018a). We find only very small variations in the radial velocities, which are on the order of the uncertainties. Based on the radial velocities, CD−28° 1974 is likely not a binary, or has a very long orbital period (tens of years or more).

We also used the UVES spectra to determine $T_{\rm eff}$ and log g. As in Reed et al. (2019) we used the spectral analysis program XTGRID (Németh et al. 2012) that builds composite spectra using LTE synthetic spectra for the companion from the BOSZ spectral library (Bohlin et al. 2017) and TLUSTY/SYNSPEC (Hubeny & Lanz 2017) non-LTE atmosphere models and synthetic spectra for the hot subdwarf. The combined synthetic spectra are then compared with an observed spectrum. The comparison is done by calculating χ^2 values and XTGRID applies iterative updates to the models to minimize χ^2 following the steepest gradient in the parameter space. In this case we fitted the least (left-hand panel of Fig. 4) and most (right-hand panel of Fig. 4) contaminated sdB spectra, to see the effect of the companion on deriving the sdB parameters. We consider the sdB parameters most secure from the least contaminated spectrum, and provide those in Table 2. To improve the fit to the least contaminated spectrum we used the information on the companion derived from the most contaminated one. The results for the most contaminated spectrum were nearly identical for the sdB with $T_{\rm eff} = 29\,790^{+1530}_{-230}$ K and log $g = 5.485^{-0.768}_{+0.002}$. As such, we consider these parameters reliable. The parameters for the MS star from the most contaminated spectrum are provided in Table 2. The Astroserver Sandbox service applies H, He, C, N, and O composition in the TLUSTY models that are appropriate to derive accurate surface parameters. We note that the UVES spectra of CD−28° 1974 show Mg II (λ4481.33 Å), Si III (λλ3806.53, 4552.628, 4567.82, 4574.76 Å), and Fe III (λλ4164.73, 4167.86, 4296.85, 4304.75, 4310.36, 4372.82, 4419.6 Å) lines, which are clearly visible in the residual in Fig. 5. Including these elements in the models would improve the results, however, this would also require better observational data.

Interestingly the fitting procedure finds the abundances of all elements included in the model, which are provided in Table 3. The lines are sufficiently strong and not too diluted by the contamination from the companion. These abundances follow the typical pattern observed in other sdB stars: helium is 0.05 solar, carbon is 0.1 solar, nitrogen is 0.5 solar, and oxygen is at 0.005 solar abundance by number. The projected rotational velocities of the components are consistent with zero and we set a rough upper limit on CD−28° 1974 of 12–15 km s^{-1} and on the companion of 5–7 km s^{-1}.

3.2 Spectral energy distribution, *Gaia*, and *TESS* light-curve analyses

We did a spectral energy distribution (SED) deconvolution fit to determine $T_{\rm eff}$ and radii of the components (Fig. 6). The deconvolution was done following the procedure outlined in Vos et al. (2018a, and references therein) with details as follows. We used photometry from the AAVSO Photometric All-Sky Survey (APASS; Henden et al. 2015), Two Micron All-Sky Survey (2MASS; Skrutskie et al. 2006), *Wide-Field Infrared Survey Explorer* (*WISE*; Cutri & et al.

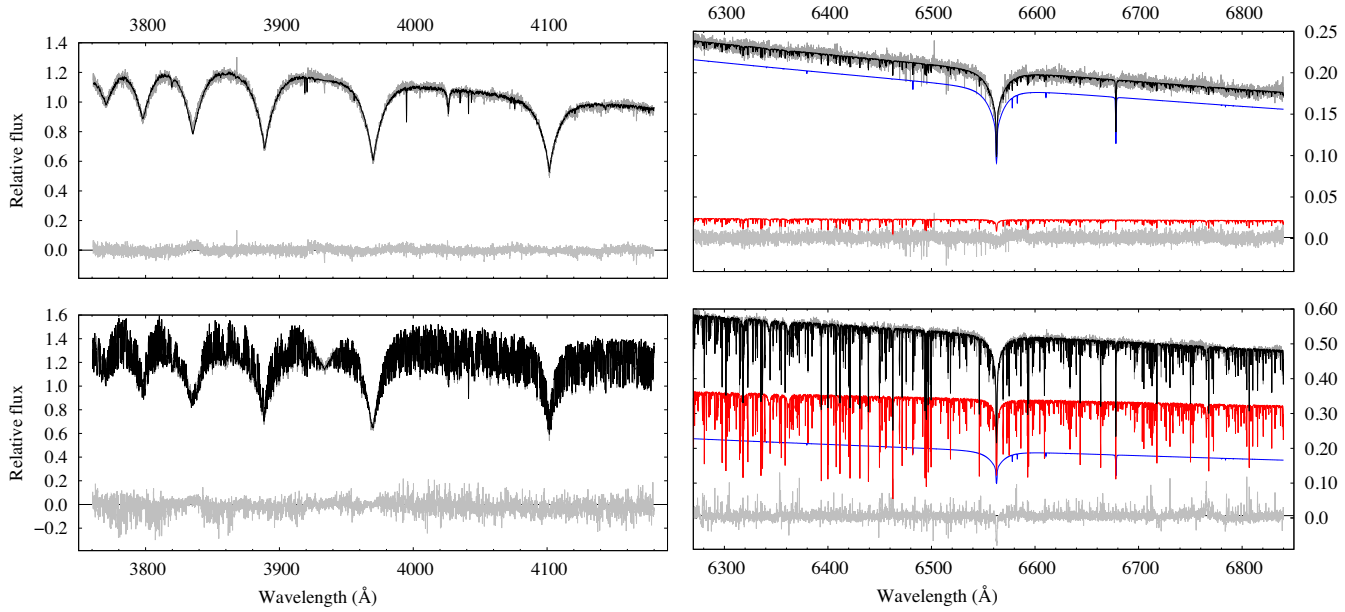

Figure 4. Comparison of the most (bottom) and least (top) contaminated spectra of CD−28° 1974. For the red part of the spectra (right) the components' models are also shown. Colours are grey for observed, black for combined model, blue for sdB model, and red for MS model. Residuals are shown in light-grey. The corresponding results from the fits are in Table 2. Both composite fits over the entire UVES range are available online at https://astroserver.org/FC6QRB/.

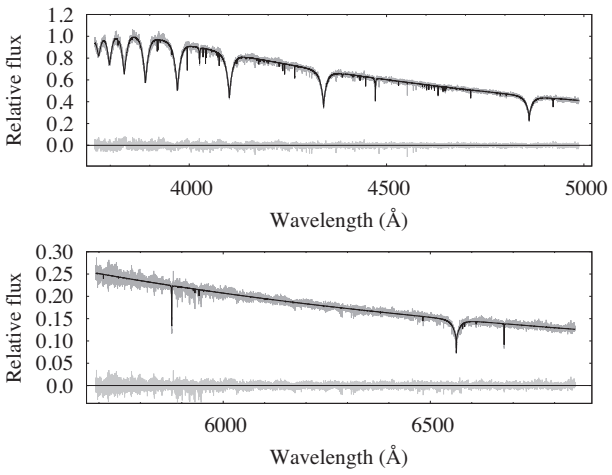

Figure 5. Best-fitting TLUSTY/XTGRID model (black) to the companion subtracted spectrum of CD−28° 1974 (grey). The observed continuum has been adjusted to the model to improve the figure.

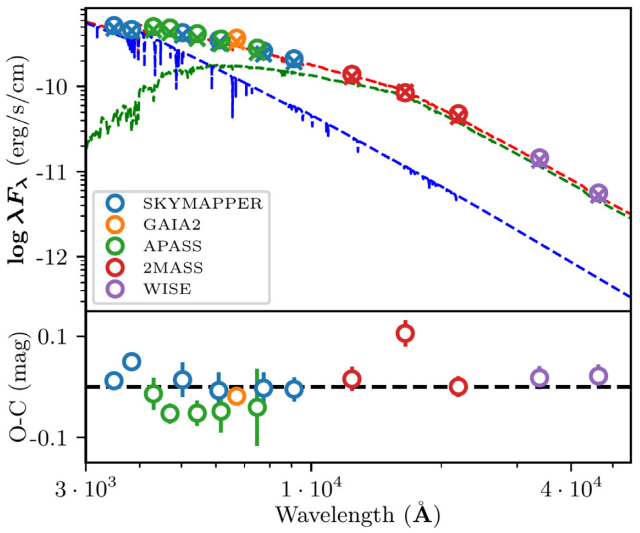

Figure 6. SED fit (top panel) including the atmospheric models (sdB in blue and MS in green) and residuals.

2012), SkyMapper (Wolf et al. 2018), and the *Gaia* G band (as only that was provided for both components; Gaia Collaboration et al. 2018; Riello et al. 2018) and an average of the *Gaia* distances. The sdB and MS model atmospheres are from Werner et al. (2003) and Kurucz (1979), respectively, and the fitting to the observations were done with EMCEE (Foreman-Mackey et al. 2013). The results are provided in Table 2.

CD−28° 1974 is resolved by *Gaia*, which shows two stars with a separation of 1.33 arcsec (Lindegren et al. 2018). Both stars have very similar proper motions and parallaxes, to within the errors, indicating that CD−28° 1974 is likely a physical pair with a very long orbital period. The *Gaia* parameters are given in Table 2. At the average distance of both components (395 ± 7 pc), the separation of this system would be 530 ± 10 au, which for an sdB+F/G binary corresponds to an orbital period on the order of 10^4 yr.

Table 3. Element abundances in CD−28° 1974.

log (nHe/nH)	−2.28 ± 0.05
log (nC/nH)	−4.44 ± 0.20
log (nN/nH)	−4.30 ± 0.15
log (nO/nH)	−5.12 ± 0.25

We examined the uncorrected light curve of CD−28° 1974 to search for signs of binarity. This could be either ellipsoidal variations or a reflection effect. Neither effect was observed. This is not surprising even if the unresolved pair is a physical binary. To our knowledge, there are no known cases of sdB stars in short-period binaries with F or G stars. Such orbits only appear to be long, with

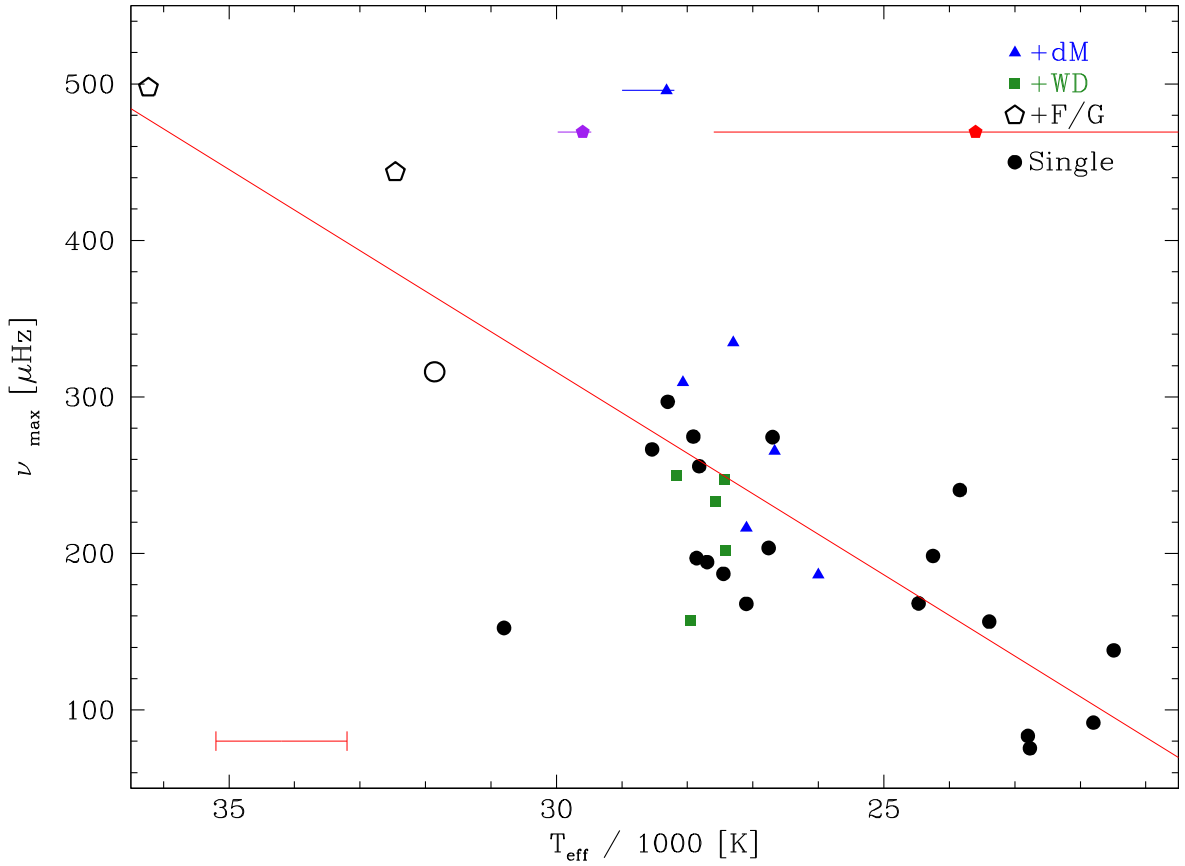

Figure 7. Comparison of effective temperature with highest amplitude *g*-mode frequency. Open points indicate *p*-mode-dominated pulsators and a trend line is indicated in red. For clarity, errors on $T_{\rm eff}$ are not shown except for CD−28° 1974 (purple from spectroscopy and red from the SED deconvolution) and EQ Psc (blue triangle; Baran et al. 2019), which are representative of typical fitting errors. An error bar is shown in the lower left indicating possible systematic differences by up to 2000 K from differing model atmospheres and fitting procedures.

periods of >100 d (Vos et al. 2013, 2018a). However, the lack of light-curve variations consistent with binarity make it unlikely there is a third star in the system.

4 DISCUSSION

From single-sector *TESS* data, we discovered CD−28° 1974 to be a new *g*-mode-dominated hybrid sdBV star and securely detect 13 periods with four others below the detection limit. All save one of the pulsations are *g* modes and five of the six highest amplitude frequencies occur between 400 and 600 μHz. All but four of the *g*-mode pulsations are associated with an $\ell = 1$ asymptotic sequence with a spacing of 268.85 ± 0.32 s. Two additional periods are associated with $\ell = 2$ modes, leaving just two *g*-mode periods without mode assignments.

4.1 CD−28° 1974's binary status

We also investigated CD−28° 1974's binary status and conclude it is most likely in a binary with a MS F/G-type star, based on *Gaia* proper motions. We also re-examined available spectroscopy and determine robust temperature and gravity placing CD−28° 1974 on the hotter end of the *g*-mode-dominated sdBV stars. We do not detect any radial velocity or light variations indicative of binarity. We cannot exclude an eccentric orbit of the F/G star, viewed near apastron, but if CD−28° 1974 is a physical binary with a very large separation, this has interesting implications. A separation of ∼500 au is too far apart for the F/G companion to influence the envelope-stripping mechanism to produce the sdB star. We do not detect indications of a third object with a shorter orbit and as such, there likely was an (or is an undetected) inner binary that produced the sdB star via a merger. These former triple systems can help to provide constraints on the time-scale of the merger event (Michaely & Perets 2019).

While MS G stars can have solar-like oscillations in a similar frequency range, such oscillations are very unlikely to be observed in *TESS* single-sector data (Campante 2017) and would have an asymptotic sequence in frequency, not period (Christensen-Dalsgaard 2018). We have ruled out oscillations from the nearby star in Section 2.3 and we attribute the oscillations to the sdB component.

4.2 CD−28° 1974's peculiar pulsations

The feature that makes CD−28° 1974 so interesting is the frequency range in which the dominant periodicities lie. Five of the six highest amplitude periodicities occur between 400 and 600 μHz. We have seen pulsations in this range before, but typically they are not the dominant amplitudes and usually high degree $\ell > 2$ (e.g. Telting et al. 2014; Foster et al. 2015) modes. That they are $\ell = 1$ modes was especially surprising to us and compelled us to examine where dominant frequencies occur in other sdBV stars. Our collaboration has examined over 40 sdBV stars from the *Kepler* mission and, except for those where no *g* modes were detected, we compared the highest amplitude frequency ($\nu_{\rm max}$) to other measurables. For

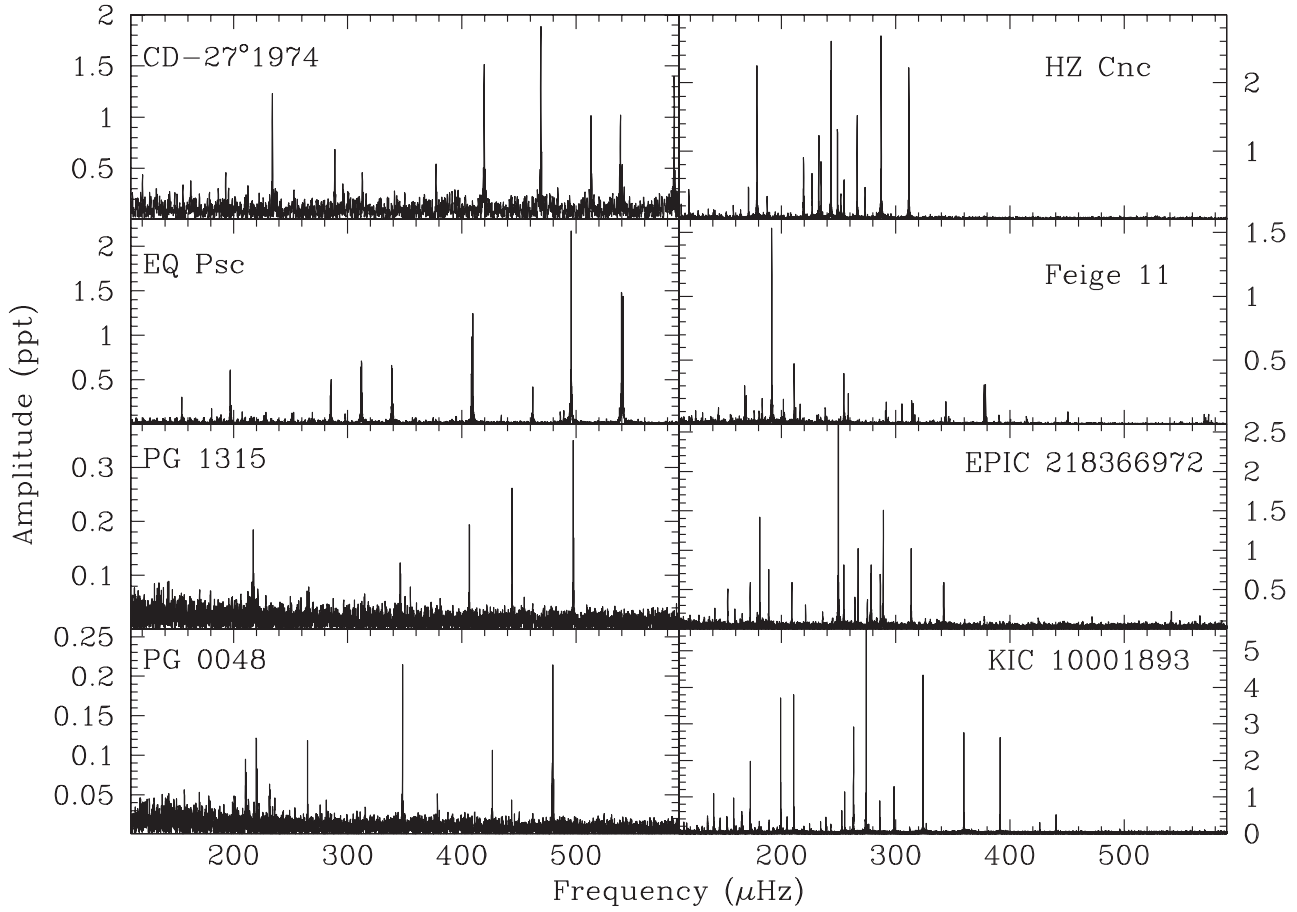

Figure 8. Comparison of FTs between higher frequency and 'typical' *g*-mode sdBV stars. Left-hand panels show the *g*-mode-dominated pulsators CD−28° 1974 and EQ Psc (top) and the *p*-mode-dominated pulsators PG 1315−123 and PG 0048+091 (bottom) that also have higher frequency *g*-mode pulsations. Except for CD−28° 1974, these FTs are all from *Kepler* mission data.

every sdBV star with identified *g* modes, $\nu_{\rm max}$ was always an $\ell = 1$ mode. Of comparisons with $T_{\rm eff}$, $\log g$, and $\Delta\Pi$, only $T_{\rm eff}$ showed a trend with $\nu_{\rm max}$.[1] We show this in Fig. 7. Besides CD−28° 1974, the *g*-mode-dominated pulsator EQ Psc also has an unusually high-frequency $\nu_{\rm max}$ (Baran et al. 2019). CD−28° 1974 and EQ Psc have similar $\log g$ and $T_{\rm eff}$, with their temperatures on the hot end of the *g*-mode pulsators. The other two stars with high-frequency $\nu_{\rm max}$ are the hotter *p*-mode-dominated stars PG 1315−123 and PG 0048+091 (Reed et al. 2019). In those stars, the *g* modes are not the highest amplitude frequencies, but rather the *p* modes are. Fig. 7 shows a general trend from upper-left to lower-right with a linear fit line. As expected, the hotter stars have the higher frequencies (shorter periods). While CD−28° 1974 and EQ Psc *roughly* fit the trend of higher $\nu_{\rm max}$ with increased $T_{\rm eff}$, they are the most deviant. Fig. 8 shows the high-frequency $\nu_{\rm max}$ stars in the left-hand panels with a sample of 'normal' $\nu_{\rm max}$ stars in the right-hand panels.

Binarity seems unlikely to play a role in the deviant $\nu_{\rm max}$s as EQ Psc is known to have a nearby M-dwarf companion while CD−28° 1974 likely has an F- or G-type companion too distant to have affected its structure. PG 1315−123 and PG 0048+091 have unresolved F-type MS companions at indeterminate distances, though likely with periods of a few years (Reed et al. 2019). Apparently 'normal' sdBV stars have all variants of companions, including no known companions (indicated by the point types in Fig. 7).

Perhaps larger $\nu_{\rm max}$ is an indicator that the core masses of CD−28° 1974 and EQ Psc differ from the ascribed canonical mass of 0.47 $M_\odot$. It has been proposed that the sdB mass distribution is related to the formation mechanism responsible for stripping off the H-rich envelope (Han et al. 2002, 2003) and so this could be an indicator of evolutionary path. Baran et al. (2019) determined a mass for EQ Psc of 0.38 ± 0.05 $M_\odot$, though they argue that their errors are most likely unrealistically small (particularly for $\log g$) and favour a canonical value. The spectroscopic analysis shows that CD−28° 1974 is a normal sdB star on the extended horizontal branch. Although the analysis is complicated by a nearby star that contaminates the spectrum of CD−28° 1974, the sdB shows a rich optical spectrum with numerous O, Mg, Si, and Fe lines. In the $T_{\rm eff}$–$\log g$ plane the sdB sits in between the two sdB groups that can be associated with clean *p*-mode or *g*-mode pulsators. A subset of stars with similar atmospheric parameters to CD−28° 1974 shows hybrid (both *p*-mode and *g*-mode) pulsations. We have not attempted a mass determination for CD−28° 1974 as the nearby star complicates *Gaia* distance determinations (Bailer-Jones et al. 2018)

[1]Most of the effective temperatures come from LTE fitting with model atmospheres as described in Østensen et al. (2010), while CD−28° 1974's is from NLTE fitting. Differences in fitting procedures and comparative atmospheric models are known to change $T_{\rm eff}$ by up to 2000 K. This will be explored further in a forthcoming publication by Reed et al.

and the discrepancies in the spectroscopic quantities will produce unacceptably large errors. Reed et al. (2019) suggested that smaller $\Delta\Pi$ values for PG 0048+091 and KIC 10139564 could be related to compact cores. CD−28° 1974 and EQ Psc have typical $\Delta\Pi$ values and KIC 10139564 has a typical $\nu_{\rm max}$ of 316 μHz. This adds to the enigmas detected in sdBV stars. The pulsations of EQ Psc and CD−28° 1974 imply there is something atypical about their structure. Here we simply report the anomaly and look forward to modelling results for an explanation.

CD−28° 1974 has turned out to be an interesting, though not quite unique sdBV star, whose analysis was made possible by space-based continuous observations over an extended time period. We anticipate other interesting surprises as *TESS* will observe nearly the entire sky, including several hundred sdB stars.

ACKNOWLEDGEMENTS

KAS was funded by the Missouri Space Grant, which is funded by NASA. JV acknowledges support from a fellowship for post-doctoral researchers awarded by the Alexander von Humboldt Foundation. PN acknowledges support from the Grant Agency of the Czech Republic (GAČR 18-20083S). This research has used the Sandbox services of www.Astroserver.org. ASB and SKS gratefully acknowledge financial support from the Polish National Science Center under projects no. UMO-2017/26/E/ST9/00703.

This study is based on observations collected at the European Organization for Astronomical Research in the Southern hemisphere under ESO programmes 088.D-0364(A) and 093.D-0629(A). This paper includes data collected by the *TESS* mission. Funding for the *TESS* mission is provided by the NASA Explorer Program. The Digitized Sky Surveys were produced at the Space Telescope Science Institute under US Government grant NAG W-2166. The images of these surveys are based on photographic data obtained using the Oschin Schmidt Telescope on Palomar Mountain and the UK Schmidt Telescope. The plates were processed into the present compressed digital form with the permission of these institutions. The National Geographic Society – Palomar Observatory Sky Atlas (POSS-I) was made by the California Institute of Technology with grants from the National Geographic Society. The Second Palomar Observatory Sky Survey (POSS-II) was made by the California Institute of Technology with funds from the National Science Foundation, the National Geographic Society, the Sloan Foundation, the Samuel Oschin Foundation, and the Eastman Kodak Corporation. The Oschin Schmidt Telescope is operated by the California Institute of Technology and Palomar Observatory. The UK Schmidt Telescope was operated by the Royal Observatory Edinburgh, with funding from the UK Science and Engineering Research Council (later the UK Particle Physics and Astronomy Research Council), until 1988 June, and thereafter by the Anglo-Australian Observatory. The blue plates of the Southern Sky Atlas and its Equatorial Extension (together known as the SERC-J), as well as the Equatorial Red (ER), and the Second Epoch [red] Survey (SES) were all taken with the UK Schmidt. All data are subject to the copyright given in the copyright summary. Copyright information specific to individual plates is provided in the downloaded FITS headers. Supplemental funding for sky survey work at the STScI is provided by the European Southern Observatory.

REFERENCES

Aerts C., Christensen-Dalsgaard J., Kurtz D. W., 2010, Asteroseismology. Springer, Netherlands
Bailer-Jones C. A. L., Rybizki J., Fouesneau M., Mantelet G., Andrae R., 2018, AJ, 156, 58
Balona L. A., Guzik J. A., Uytterhoeven K., Smith J. C., Tenenbaum P., Twicken J. D., 2011, MNRAS, 415, 3531
Balona L. A., Daszyńska-Daszkiewicz J., Pamyatnykh A. A., 2015, MNRAS, 452, 3073
Baran A. S., Winans A., 2012, Acta Astron., 62, 343
Baran A. S. et al., 2012, MNRAS, 424, 2686
Baran A. S., Telting J. H., Jeffery C. S., Østensen R. H., Vos J., Reed M. D., Vučković M., 2019, MNRAS, 489, 1556
Bohlin R. C., Mészáros S., Fleming S. W., Gordon K. D., Koekemoer A. M., Kovács J., 2017, AJ, 153, 234
Campante T. L., 2017, EPJ Web Conf., 160, 01006
Christensen-Dalsgaard J., 2018, in Rozelot J.-P., ed., Variability of the Sun and Sun-like Stars: From Asteroseismology to Space Weather. Springer-Verlag, Berlin, p. 125
Cutri R. M. et al., 2012, VizieR On-line Data Catalog: II/311
Foreman-Mackey D., Hogg D. W., Lang D., Goodman J., 2013, PASP, 125, 306
Foster H. M., Reed M. D., Telting J. H., Østensen R. H., Baran A. S., 2015, ApJ, 805, 94
Gaia Collaboration et al., 2018, A&A, 616, A1
García R. A., Ballot J., 2019, Living Rev. Sol. Phys., 16, 4
Han Z., Podsiadlowski P., Maxted P. F. L., Marsh T. R., Ivanova N., 2002, MNRAS, 336, 449
Han Z., Podsiadlowski P., Maxted P. F. L., Marsh T. R., 2003, MNRAS, 341, 669
Heber U., 2016, PASP, 128, 082001
Henden A. A., Levine S., Terrell D., Welch D. L., 2015, Am. Astron. Soc. Meeting Abstr., #225, 336
Hubeny I., Lanz T., 2017, preprint (arXiv:1706.01937)
Kurucz R. L., 1979, ApJS, 40, 1
Lindegren L. et al., 2018, A&A, 616, A2
Michaely E., Perets H. B., 2019, MNRAS, 484, 4711
Németh P., Kawka A., Vennes S., 2012, MNRAS, 427, 2180
Østensen R. H. et al., 2010, MNRAS, 409, 1470
Reed M. D. et al., 2011, MNRAS, 414, 2885
Reed M. D. et al., 2018, Open Astron., 27, 157
Reed M. D. et al., 2019, MNRAS, 483, 2282
Ricker G. R., 2015, AAS/Division Extreme Sol. Syst. Abstr., 503
Ricker G. R. et al., 2016, Proc. SPIE, 9904, 99042B
Riello M. et al., 2018, A&A, 616, A3
Skrutskie M. F. et al., 2006, AJ, 131, 1163
Telting J. H. et al., 2014, A&A, 570, A129
Vennes S., Kawka A., Németh P., 2011, MNRAS, 410, 2095
Vos J., Østensen R. H., Németh P., Green E. M., Heber U., Van Winckel H., 2013, A&A, 559, A54
Vos J., Østensen R. H., Vuckovic M., Telting J. H., 2018a, A&A, 842, 78
Vos J., Németh P., Vučković M., Østensen R., Parsons S., 2018b, MNRAS, 473, 693
Werner K., Deetjen J. L., Dreizler S., Nagel T., Rauch T., Schuh S. L., 2003, in Hubeny I., Mihalas D., Werner K., eds, ASP Conf. Ser. Vol. 288, Stellar Atmosphere Modeling. Astron. Soc. Pac., San Francisco, p. 31
Wolf C. et al., 2018, Publ. Astron. Soc. Aust., 35, e010

This paper has been typeset from a TEX/LATEX file prepared by the author.